PERGAMON

International Journal of Heat and Mass Transfer 46 (2003) 551–563

International Journal of HEAT and MASS TRANSFER

www.elsevier.com/locate/ijhmt

Time-periodic laminar mixed convection in an inclined channel

A. Barletta *, E. Zanchini

Dipartimento di Ingegneria Energetica, Nucleare e del Controllo Ambientale (DIENCA), Università di Bologna, Viale Risorgimento 2, I-40136 Bologna, Italy

Received 17 January 2002; received in revised form 24 May 2002

Abstract

The steady-periodic regime of laminar mixed convection in an inclined channel is studied analytically, with the following boundary conditions: the temperature of one channel wall is stationary, while the temperature of the other wall is a sinusoidal function of time. Analytical expressions of the velocity field, of the temperature field, of the pressure drop, of the friction factors, as well as of the Nusselt number at any plane parallel to the walls are determined. It is found that, for every value of the Prandtl number greater than 0.277, there exists a resonance frequency which maximizes the amplitude of the friction factor oscillations at the unsteady-temperature wall. Moreover, for any plane which lies between the midplane of the channel and the unsteady-temperature wall, every value of the Prandtl number yields a resonance frequency which maximizes the amplitude of the Nusselt number oscillations.

Keywords: Laminar flow; Unsteady mixed convection; Inclined duct; Analytical methods

1. Introduction

Many analytical studies on fully developed laminar mixed convection in either vertical or inclined channels are available in the literature. These studies refer to steady flows, and provide analytical solutions for different boundary conditions. The viscous dissipation in the fluid is either neglected [1–5] or considered [6–9]. On the other hand, numerical methods have been employed to investigate the steady-periodic natural convection in a square enclosure with both the upper and the lower wall insulated, and the left vertical wall kept at a constant temperature. Two boundary conditions for the right vertical wall have been considered: a uniform temperature which varies in time with a sinusoidal law [10,11], a uniform heat flux which varies periodically in time with square-wave pulses [12,13]. In Refs. [11–13], a resonance phenomenon has been predicted: the heat flux through a vertical surface fluctuates with an amplitude that, for fixed values of the other parameters, reaches a maximum for a given value of the angular frequency, called resonance frequency. In Refs. [10,11], different results have been obtained concerning the time-averaged heat transfer across the enclosure. In Ref. [10] this quantity has been found to be rather insensitive to the time-dependent boundary conditions. On the other hand, the results obtained in Ref. [11] show that a large-amplitude wall temperature oscillation causes an increase of the time-averaged heat transfer rate and that the increase is maximum at a resonance frequency.

In this paper, the time-periodic laminar mixed convection in an inclined channel is studied analytically with the following boundary conditions: the temperature of one wall is constant, while that of the other wall is a sinusoidal function of time. Thus, the results obtained in Refs. [1–5] are extended to the case of steady-periodic conditions. Moreover, the numerical investigations presented in Refs. [10–13] are complemented by the analytical study of similar phenomena in a simpler geometry. The results allow one to describe the oscillations of the dimensionless velocity, of the dimensionless temperature, of the dimensionless pressure drop, of the friction factors, of the dimensionless heat flux

* Corresponding author. Tel.: +390-51-209-3295; fax: +390-51-209-3296.
E-mail address: antonio.barletta@mail.ing.unibo.it (A. Barletta).

0017-9310/03/$ - see front matter
PII: S0017-9310(02)00290-9

Nomenclature

A, B	functions defined by Eq. (9)
D	hydraulic diameter, $4L$
f_1	Fanning friction factor at the wall $Y = -L$, defined in Eq. (21)
f_2	Fanning friction factor at the wall $Y = L$, defined in Eq. (21)
f_{1a}^*, f_{1b}^*	complex functions defined by Eq. (39)
f_{2a}^*, f_{2b}^*	complex functions defined by Eq. (40)
$\mathbf{g}$	gravitational acceleration
g	magnitude of the gravitational acceleration
G	dimensionless complex function defined by Eq. (32)
Gr	Grashof number, defined in Eq. (11)
k	thermal conductivity
L	half of the channel width
Nu	Nusselt number defined by Eq. (34)
Nu^*, Nu_a^*, Nu_b^*	dimensionless complex functions defined by Eqs. (35) and (36)
p	pressure
P	difference between the pressure and the hydrostatic pressure, $p + \varrho_0 g(X\cos\varphi - Y\sin\varphi)$
Pr	Prandtl number, defined in Eq. (11)
q	heat flux per unit area
$\mathscr{R}e$	real part of a complex number
Re	Reynolds number, defined in Eq. (11)
t	time
T	temperature
T_0	average temperature in a channel section
T_1	temperature of the wall $Y = -L$
T_2	time-averaged temperature of the wall $Y = L$
u	dimensionless velocity defined in Eq. (11)
$\mathbf{U}$	velocity
U	X-component of the fluid velocity
u^*, u_a^*, u_b^*	dimensionless complex functions defined by Eqs. (23) and (24)
U_0	average velocity in a channel section
X, Y	rectangular coordinates
y	dimensionless coordinate defined in Eq. (11)

Greek symbols

α	thermal diffusivity
β	volumetric coefficient of thermal expansion
Γ	dimensionless complex parameter defined in Eq. (31)
ΔT	amplitude of the temperature oscillations at $Y = L$
η	dimensionless time, defined in Eq. (11)
θ	dimensionless temperature, defined in Eq. (11)
θ^*, θ_a^*, θ_b^*	dimensionless complex functions defined by Eqs. (23) and (24)
λ	dimensionless pressure drop, defined in Eq. (11)
λ^*, λ_a^*, λ_b^*	dimensionless complex functions defined in Eqs. (23) and (24)
μ	dynamic viscosity
ν	kinematic viscosity
ξ	dimensionless parameter defined in Eq. (11)
ϱ	mass density
ϱ_0	mass density for $T = T_0$
φ	tilt angle
χ	dimensionless parameter defined in Eq. (11)
ω	angular frequency
Ω	dimensionless angular frequency, defined in Eq. (11)

through any plane parallel to the walls. It is found that, for sufficiently high values of the Prandtl number, there exists a resonance frequency which maximizes the oscillation amplitude of the friction factor at the unsteady-temperature wall. Moreover, for every value of the Prandtl number, a resonance frequency for the oscillation amplitude of the dimensionless heat flux exists for any plane which lies between the midplane of the channel and the unsteady-temperature wall, while the time-averaged heat flux is independent of the temperature oscillations.

2. Mathematical model

Let us consider the laminar flow of a Newtonian fluid in the gap between two infinitely-wide plane parallel walls. The flow is assumed to be parallel such that **U** has the only non-vanishing component U along the X-axis. The axis orthogonal to the walls, the gravitational acceleration **g** and the X-axis lie on the same plane. The latter condition ensures that the flow can be considered as two-dimensional, i.e. both the velocity field and the temperature field depend only on two spatial coordinates. The system under consideration is sketched in Fig. 1, where the chosen coordinate axes (X, Y) are drawn. Let us assume that the wall at $Y = -L$ is kept isothermal with a constant temperature T_1, while the wall at $Y = L$ is subjected to an oscillating temperature

$$T(X, L, t) = T_2 + \Delta T \cos(\omega t). \tag{1}$$

Moreover, heat flow is assumed to occur only in the transverse direction, so that $\partial T/\partial X = 0$. The latter assumption is conceivable since each wall is kept at a uniform temperature. The Boussinesq approximation is invoked, so that **U** is a solenoidal field and, as a consequence, $\partial U/\partial X = 0$. A steady mass flow rate is prescribed; therefore the average velocity in a channel section, defined as

$$U_0 = \frac{1}{2L}\int_{-L}^{L} U \,\mathrm{d}Y, \tag{2}$$

is time independent.

The equation of state, $\varrho = \varrho(T)$ is considered as linear,

$$\varrho = \varrho_0[1 - \beta(T - T_0)], \tag{3}$$

where T_0 is an average temperature both with respect to the interval $-L \leqslant Y \leqslant L$ and to the period $0 \leqslant t \leqslant 2\pi/\omega$, namely

$$T_0 = \frac{\omega}{4\pi L}\int_0^{2\pi/\omega} \mathrm{d}t \int_{-L}^{L} \mathrm{d}Y\, T. \tag{4}$$

Obviously, since $\partial T/\partial X = 0$, the reference temperature T_0 is a constant. According to the Boussinesq approximation, the momentum balance equation yields, along the X and Y axes,

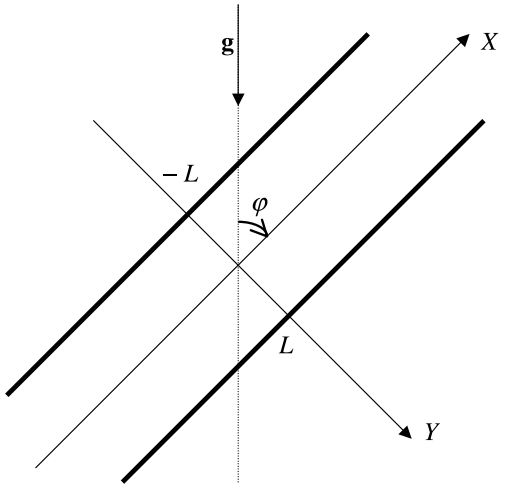

Fig. 1. Drawing of the channel and of the coordinate axes.

$$\varrho_0 \frac{\partial U}{\partial t} = \varrho_0 g\beta(T - T_0)\cos\varphi - \frac{\partial P}{\partial X} + \mu \frac{\partial^2 U}{\partial Y^2}, \tag{5}$$

$$\varrho_0 g\beta(T - T_0)\sin\varphi + \frac{\partial P}{\partial Y} = 0, \tag{6}$$

where $P = p + \varrho_0 g(X\cos\varphi - Y\sin\varphi)$. If both sides of Eq. (5) are derived with respect to X, one obtains

$$\frac{\partial^2 P}{\partial X^2} = 0. \tag{7}$$

Moreover, if both sides of Eq. (6) are derived with respect to X, one obtains

$$\frac{\partial^2 P}{\partial X \partial Y} = 0. \tag{8}$$

It is easily verified that Eqs. (8) and (9) imply the existence of two functions $A(Y,t)$ and $B(t)$ such that

$$P(X,Y,t) = A(Y,t) - B(t)X. \tag{9}$$

The energy balance equation is given by

$$\frac{\partial T}{\partial t} = \alpha \frac{\partial^2 T}{\partial Y^2}. \tag{10}$$

Let us define the dimensionless quantities

$$\theta = \frac{T - T_0}{\Delta T}, \quad u = \frac{U}{U_0}, \quad y = \frac{Y}{D}, \quad \eta = \omega t, \quad \lambda = \frac{D^2 B}{\mu U_0}, \quad \Omega = \frac{\omega D^2}{\nu}, \quad Pr = \frac{\nu}{\alpha}, \quad Re = \frac{U_0 D}{\nu}, \quad Gr = \frac{g\beta\Delta T D^3 \cos\varphi}{\nu^2},$$
$$\chi = \frac{T_2 - T_1}{\Delta T}, \quad \xi = \frac{T_1 - T_0}{\Delta T}, \tag{11}$$

where $D = 4L$ is the hydraulic diameter. By employing Eqs. (9) and (11), Eqs. (5) and (10) can be rewritten as

$$\Omega \frac{\partial u}{\partial \eta} = \frac{Gr}{Re}\theta + \lambda + \frac{\partial^2 u}{\partial y^2}, \tag{12}$$

$$\frac{\partial \theta}{\partial \eta} = \frac{1}{\Omega Pr}\frac{\partial^2 \theta}{\partial y^2}. \tag{13}$$

The no slip condition at the walls implies that

$$u(-1/4,\eta) = 0 = u(1/4,\eta), \tag{14}$$

while the dimensionless thermal boundary conditions are

$$\theta(-1/4,\eta) = \xi, \tag{15}$$

$$\theta(1/4,\eta) = \xi + \chi + \cos\eta. \tag{16}$$

Eqs. (2) and (4) imply the following constraints on the functions $u(y,\eta)$ and $\theta(y,\eta)$:

$$\int_{-1/4}^{1/4} u(y,\eta)\,\mathrm{d}y = \frac{1}{2}, \tag{17}$$

$$\int_0^{2\pi} \mathrm{d}\eta \int_{-1/4}^{1/4} \mathrm{d}y\,\theta(y,\eta) = 0. \tag{18}$$

Obviously, Eq. (17) yields the further constraint

$$\int_{-1/4}^{1/4} \frac{\partial u(y,\eta)}{\partial \eta}\,\mathrm{d}y = 0. \tag{19}$$

On account of Eq. (19), an integration of Eq. (12) with respect to y in the range [−1/4, 1/4] yields

$$\left.\frac{\partial u}{\partial y}\right|_{y=-1/4} - \left.\frac{\partial u}{\partial y}\right|_{y=1/4} = \frac{\lambda}{2} + \frac{Gr}{Re}\int_{-1/4}^{1/4}\theta(y,\eta)\,\mathrm{d}y. \tag{20}$$

The friction factors f_1 and f_2 at the walls $Y=-L$ and $Y=L$ respectively are defined as

$$f_1 = \frac{2\nu}{U_0^2}\left.\frac{\partial U}{\partial Y}\right|_{Y=-L} = \frac{2}{Re}\left.\frac{\partial u}{\partial y}\right|_{y=-1/4}, \quad f_2 = -\frac{2\nu}{U_0^2}\left.\frac{\partial U}{\partial Y}\right|_{Y=L} = -\frac{2}{Re}\left.\frac{\partial u}{\partial y}\right|_{y=1/4}. \tag{21}$$

On account of Eq. (20), the friction factors and the parameter λ are related as follows:

$$(f_1+f_2)Re = \lambda + 2\frac{Gr}{Re}\int_{-1/4}^{1/4}\theta(y,\eta)\,\mathrm{d}y. \tag{22}$$

3. Analytical solution, for steady periodic regime

Since Eqs. (12)–(18) are linear, one can define the complex valued functions $u^*(y,\eta)$, $\theta^*(y,\eta)$, $\lambda^*(\eta)$, which fulfil the equations

$$\begin{aligned}
&\Omega\frac{\partial u^*}{\partial \eta} = \frac{Gr}{Re}\theta^* + \lambda^* + \frac{\partial^2 u^*}{\partial y^2},\\
&\frac{\partial \theta^*}{\partial \eta} = \frac{1}{\Omega Pr}\frac{\partial^2\theta^*}{\partial y^2},\\
&u^*(-1/4,\eta) = 0 = u^*(1/4,\eta),\\
&\theta^*(-1/4,\eta) = \xi, \quad \theta^*(1/4,\eta) = \xi + \chi + \mathrm{e}^{\mathrm{i}\eta},\\
&\int_{-1/4}^{1/4} u^*(y,\eta)\,\mathrm{d}y = \frac{1}{2},\\
&\int_0^{2\pi}\mathrm{d}\eta\int_{-1/4}^{1/4}\mathrm{d}y\,\theta^*(y,\eta) = 0,
\end{aligned} \tag{23}$$

and are such that $u = \mathscr{R}e(u^*)$, $\theta = \mathscr{R}e(\theta^*)$, $\lambda = \mathscr{R}e(\lambda^*)$. In steady-periodic regime, a solution of Eq. (23) can be written in the form

$$\begin{aligned}
&u^*(y,\eta) = u_{\mathrm{a}}^*(y) + \frac{Gr}{Re}u_{\mathrm{b}}^*(y)\mathrm{e}^{\mathrm{i}\eta},\\
&\theta^*(y,\eta) = \theta_{\mathrm{a}}^*(y) + \theta_{\mathrm{b}}^*(y)\mathrm{e}^{\mathrm{i}\eta},\\
&\lambda^*(\eta) = \lambda_{\mathrm{a}}^* + \frac{Gr}{Re}\lambda_{\mathrm{b}}^*\mathrm{e}^{\mathrm{i}\eta}.
\end{aligned} \tag{24}$$

Due to the linearity of Eq. (23), if one substitutes Eq. (24) into Eq. (23) one obtains two distinct boundary value problems. The first is given by

$$\begin{aligned}
&\frac{\mathrm{d}^2 u_{\mathrm{a}}^*}{\mathrm{d}y^2} + \frac{Gr}{Re}\theta_{\mathrm{a}}^* + \lambda_{\mathrm{a}}^* = 0,\\
&\frac{\mathrm{d}^2\theta_{\mathrm{a}}^*}{\mathrm{d}y^2} = 0,\\
&u_{\mathrm{a}}^*(-1/4) = 0 = u_{\mathrm{a}}^*(1/4),\\
&\theta_{\mathrm{a}}^*(-1/4) = \xi, \quad \theta_{\mathrm{a}}^*(1/4) = \xi + \chi,\\
&\int_{-1/4}^{1/4} u_{\mathrm{a}}^*(y)\,\mathrm{d}y = \frac{1}{2},\\
&\int_{-1/4}^{1/4}\theta_{\mathrm{a}}^*(y)\,\mathrm{d}y = 0;
\end{aligned} \tag{25}$$

while the second is given by

$$\begin{aligned}
&\frac{\mathrm{d}^2 u_{\mathrm{b}}^*}{\mathrm{d}y^2} - i\Omega u_{\mathrm{b}}^* + \theta_{\mathrm{b}}^* + \lambda_{\mathrm{b}}^* = 0,\\
&\frac{\mathrm{d}^2 \theta_{\mathrm{b}}^*}{\mathrm{d}y^2} - i\Omega Pr\,\theta_{\mathrm{b}}^* = 0,\\
&u_{\mathrm{b}}^*(-1/4) = 0 = u_{\mathrm{b}}^*(1/4),\\
&\theta_{\mathrm{b}}^*(-1/4) = 0, \quad \theta_{\mathrm{b}}^*(1/4) = 1,\\
&\int_{-1/4}^{1/4} u_{\mathrm{b}}^*(y)\,\mathrm{d}y = 0.
\end{aligned} \tag{26}$$

The differential equations and the boundary conditions which appear in Eq. (25) yield the distributions $u_{\mathrm{a}}^*(y)$ and $\theta_{\mathrm{a}}^*(y)$ as functions of the unknown parameters λ_{a}^* and ξ. Then, these parameters can be determined by employing the integral constraints on $u_{\mathrm{a}}^*(y)$ and $\theta_{\mathrm{a}}^*(y)$ given in Eq. (25). For instance, the constraint on $\theta_{\mathrm{a}}^*(y)$ yields $\xi = -\chi/2$ which, on account of Eq. (11), implies $T_0 = (T_1 + T_2)/2$. The solution of Eq. (25) is as follows:

$$\begin{aligned}
&\theta_{\mathrm{a}}^*(y) = 2\chi y, \quad \lambda_{\mathrm{a}}^* = 48,\\
&u_{\mathrm{a}}^*(y) = \frac{1}{48}(1 - 16y^2)\left(72 + \chi\frac{Gr}{Re}y\right).
\end{aligned} \tag{27}$$

With reference to Eq. (26), the differential equations and the boundary conditions yield the distributions $u_{\mathrm{b}}^*(y)$ and $\theta_{\mathrm{b}}^*(y)$ as functions of the unknown parameter λ_{b}^*. The latter parameter is determined by means of the integral constraint which appears in Eq. (26), so that the solution of this equation is given by

$$\theta_{\mathrm{b}}^*(y) = (\mathrm{e}^{\Gamma} - 1)^{-1}\left\{\exp\left[\left(\frac{3}{4} + y\right)\Gamma\right] - \exp\left[\left(\frac{1}{4} - y\right)\Gamma\right]\right\}, \tag{28}$$

$$\begin{aligned}
\lambda_{\mathrm{b}}^* = {} & 2\left\{\left[1 - \exp\left(\frac{\Gamma}{2} + \frac{\Gamma}{2\sqrt{Pr}}\right)\right]\left(\sqrt{Pr} - 1\right) + \left[\mathrm{e}^{\Gamma/2} - \exp\left(\frac{\Gamma}{2\sqrt{Pr}}\right)\right]\left(\sqrt{Pr} + 1\right)\right\}\left[1 + \exp\left(\frac{\Gamma}{2}\right)\right]^{-1}(Pr - 1)^{-1}\\
& \times \left[4\sqrt{Pr} + \Gamma - \exp\left(\frac{\Gamma}{2\sqrt{Pr}}\right)\left(4\sqrt{Pr} - \Gamma\right)\right]^{-1}.
\end{aligned} \tag{29}$$

$$u_{\mathrm{b}}^*(y) = \frac{Pr}{\Gamma^2(Pr - 1)}\exp\left[-\left(2 + \frac{1}{\sqrt{Pr}}\right)y\Gamma\right](\mathrm{e}^{\Gamma} - 1)^{-1}\left[\exp\left(\frac{\Gamma}{\sqrt{Pr}}\right) - 1\right]^{-1} G(y). \tag{30}$$

In Eqs. (28)–(30), the parameter Γ is defined as

$$\Gamma = \sqrt{i\Omega Pr}, \tag{31}$$

while the function $G(y)$ is given by

$$\begin{aligned}
G(y) = {} & \exp\left[\frac{3\Gamma}{4} + \left(3 + \frac{1}{\sqrt{Pr}}\right)y\Gamma\right] - \exp\left[\frac{\Gamma}{4} + \left(1 + \frac{1}{\sqrt{Pr}}\right)y\Gamma\right] + \exp\left[\frac{\Gamma}{4} + \frac{\Gamma}{\sqrt{Pr}} + \left(1 + \frac{1}{\sqrt{Pr}}\right)y\Gamma\right]\\
& - \exp\left[\frac{3\Gamma}{4} + \frac{\Gamma}{\sqrt{Pr}} + \left(3 + \frac{1}{\sqrt{Pr}}\right)y\Gamma\right] + \lambda_{\mathrm{b}}^*(Pr - 1)\left(1 - \mathrm{e}^{\Gamma}\right)\exp\left[\left(2 + \frac{1}{\sqrt{Pr}}\right)y\Gamma\right] - \lambda_{\mathrm{b}}^*(Pr - 1)\\
& \times \exp\left[\frac{1 + 8\left(1 + \sqrt{Pr}\right)y}{4\sqrt{Pr}}\Gamma\right] - \lambda_{\mathrm{b}}^*(Pr - 1)\exp\left[\frac{1 + \left(1 + 2\sqrt{Pr}\right)y}{\sqrt{Pr}}\Gamma\right] + \lambda_{\mathrm{b}}^*(Pr - 1)\exp\left[\frac{4\sqrt{Pr} + 1}{4\sqrt{Pr}}\Gamma\right.\\
& \left. + 2\frac{\sqrt{Pr} + 1}{\sqrt{Pr}}y\Gamma\right] + \lambda_{\mathrm{b}}^*(Pr - 1)\exp\left[\frac{\left(\sqrt{Pr} + 1\right)\Gamma + \left(2\sqrt{Pr} + 1\right)y\Gamma}{\sqrt{Pr}}\right] + \lambda_{\mathrm{b}}^*(Pr - 1)\exp\left[\frac{3\Gamma}{4\sqrt{Pr}} + 2y\Gamma\right]\\
& - \lambda_{\mathrm{b}}^*(Pr - 1)\exp\left[\Gamma + \frac{3\Gamma}{4\sqrt{Pr}} + 2y\Gamma\right] + \left[\lambda_{\mathrm{b}}^*(Pr - 1) - 1\right]\exp\left[\frac{3\Gamma + 8\left(\sqrt{Pr} + 1\right)y\Gamma}{4\sqrt{Pr}}\right] + \left[\lambda_{\mathrm{b}}^*(Pr - 1) - 1\right]\\
& \times \exp\left[\Gamma + \frac{\Gamma}{4\sqrt{Pr}} + 2y\Gamma\right] + \left[1 - \lambda_{\mathrm{b}}^*(Pr - 1)\right]\exp\left[\Gamma + \frac{3\Gamma}{4\sqrt{Pr}} + 2\frac{\sqrt{Pr} + 1}{\sqrt{Pr}}y\Gamma\right] + \left[1 - \lambda_{\mathrm{b}}^*(Pr - 1)\right]\\
& \times \exp\left[\frac{\Gamma}{4\sqrt{Pr}} + 2y\Gamma\right].
\end{aligned} \tag{32}$$

By employing Eq. (11), the heat flux per unit area can be written as

$$q = k\frac{\partial T}{\partial Y} = \frac{k\Delta T}{D}\frac{\partial \theta}{\partial y}. \tag{33}$$

In analogy with the literature [10–13], we will define a dimensionless heat flux per unit area, called Nusselt number, as follows:

$$Nu = \frac{qD}{k\Delta T} = \frac{\partial \theta}{\partial y} = \mathscr{R}e\left(\frac{\partial \theta^*}{\partial y}\right) = \mathscr{R}e(Nu^*), \tag{34}$$

where, on account of Eq. (24), Nu^* is defined as

$$Nu^* = \frac{\partial \theta^*_{\rm a}}{\partial y} + \frac{\partial \theta^*_{\rm b}}{\partial y}\mathrm{e}^{\mathrm{i}\eta} = Nu^*_{\rm a} + Nu^*_{\rm b}\mathrm{e}^{\mathrm{i}\eta}. \tag{35}$$

As a consequence of Eqs. (27) and (28), the quantities $Nu^*_{\rm a}$ and $Nu^*_{\rm b}$ employed in Eq. (35) are given by

$$\begin{aligned} &Nu^*_{\rm a} = 2\chi, \\ &Nu^*_{\rm b} = \Gamma(\mathrm{e}^{\Gamma}-1)^{-1}\left\{\exp\left[\left(\frac{3}{4}+y\right)\Gamma\right] + \exp\left[\left(\frac{1}{4}-y\right)\Gamma\right]\right\}. \end{aligned} \tag{36}$$

Eqs. (35) and (36) point out that the mean value in a period of the Nusselt number is given by $Nu^*_{\rm a}$ and depends only on χ, i.e., is independent of y, Ω and Pr. On the contrary, the amplitude of the fluctuations of the Nusselt number is given by the modulus of $Nu^*_{\rm b}$ and depends on y and on the product ΩPr.

Finally, Eqs. (21) and (24) allow one to express the quantities f_1Re and f_2Re as

$$f_1Re = 2\mathscr{R}e\left(\left.\frac{\partial u^*_{\rm a}}{\partial y}\right|_{y=-1/4} + \frac{Gr}{Re}\left.\frac{\partial u^*_{\rm b}}{\partial y}\right|_{y=-1/4}\mathrm{e}^{\mathrm{i}\eta}\right) = \mathscr{R}e\left(f^*_{1\rm a}Re + \frac{Gr}{Re}f^*_{1\rm b}Re\,\mathrm{e}^{\mathrm{i}\eta}\right), \tag{37}$$

$$f_2Re = -2\mathscr{R}e\left(\left.\frac{\partial u^*_{\rm a}}{\partial y}\right|_{y=1/4} + \frac{Gr}{Re}\left.\frac{\partial u^*_{\rm b}}{\partial y}\right|_{y=1/4}\mathrm{e}^{\mathrm{i}\eta}\right) = \mathscr{R}e\left(f^*_{2\rm a}Re + \frac{Gr}{Re}f^*_{2\rm b}Re\,\mathrm{e}^{\mathrm{i}\eta}\right), \tag{38}$$

where $f^*_{1\rm a}Re$, $f^*_{1\rm b}Re$, $f^*_{2\rm a}Re$ and $f^*_{2\rm b}Re$ are given by

$$f^*_{1\rm a}Re = 2\left.\frac{\partial u^*_{\rm a}}{\partial y}\right|_{y=-1/4}, \quad f^*_{1\rm b}Re = 2\left.\frac{\partial u^*_{\rm b}}{\partial y}\right|_{y=-1/4}, \tag{39}$$

$$f^*_{2\rm a}Re = -2\left.\frac{\partial u^*_{\rm a}}{\partial y}\right|_{y=1/4}, \quad f^*_{2\rm b}Re = -2\left.\frac{\partial u^*_{\rm b}}{\partial y}\right|_{y=1/4}. \tag{40}$$

Eqs. (27), (39) and (40) yield

$$\begin{aligned} &f^*_{1\rm a}Re = 24 - \frac{\chi}{12}\frac{Gr}{Re}, \\ &f^*_{2\rm a}Re = 24 + \frac{\chi}{12}\frac{Gr}{Re}. \end{aligned} \tag{41}$$

The expressions of $f^*_{1\rm b}Re$ and $f^*_{2\rm b}Re$ can be obtained from Eqs. (30), (39) and (40), namely

$$\begin{aligned} f^*_{1\rm b}Re = {} & \frac{2Pr}{\Gamma^2(Pr-1)}\exp\left[\left(2+\frac{1}{\sqrt{Pr}}\right)\frac{\Gamma}{4}\right](\mathrm{e}^{\Gamma}-1)^{-1}\left[\exp\left(\frac{\Gamma}{\sqrt{Pr}}\right)-1\right]^{-1} \\ & \times\left[\left.\frac{\mathrm{d}G(y)}{\mathrm{d}y}\right|_{y=-1/4} - \left(2+\frac{1}{\sqrt{Pr}}\right)\Gamma G(-1/4)\right], \end{aligned} \tag{42}$$

$$\begin{aligned} f^*_{2\rm b}Re = {} & -\frac{2Pr}{\Gamma^2(Pr-1)}\exp\left[-\left(2+\frac{1}{\sqrt{Pr}}\right)\frac{\Gamma}{4}\right](\mathrm{e}^{\Gamma}-1)^{-1}\left[\exp\left(\frac{\Gamma}{\sqrt{Pr}}\right)-1\right]^{-1} \\ & \times\left[\left.\frac{\mathrm{d}G(y)}{\mathrm{d}y}\right|_{y=1/4} - \left(2+\frac{1}{\sqrt{Pr}}\right)\Gamma G(1/4)\right]. \end{aligned} \tag{43}$$

4. Discussion of the results: pressure drop, friction factors and Nusselt number

As is shown by Eq. (27), the steady part λ_a^* of the complex pressure drop coefficient λ^* is a real constant and coincides with the dimensionless pressure drop coefficient λ obtained in the analysis of the steady case [1,5,9]. Moreover, Eqs. (24) and (29) show that the oscillating part is proportional to Gr/Re and to the complex quantity λ_b^*, which depends on Ω and Pr. Since the dimensionless pressure drop coefficient λ coincides with the real part of λ^*, the amplitude of the oscillations of λ is equal to $|\lambda_b^*|Gr/Re$. Plots of the modulus of λ_b^* versus Ω in the range $0 \leqslant \Omega \leqslant 100$ are reported in Fig. 2, for $Pr = 0.7$, 7 and 100. The figure shows that the amplitude of the fluctuations of the pressure drop coefficient λ is a decreasing function of Ω, for every value of Pr, and that the decrease is faster for higher values of Pr. As it can be inferred from Eqs. (37) and (38), the amplitudes of the oscillations of the friction factors f_1 and f_2 are given by $|f_{1b}^* Gr/Re|$ and $|f_{2b}^* Gr/Re|$, respectively. The amplitude of the oscillations of $f_1 Re^2/Gr$, i.e. $|f_{1b}^* Re|$, is a decreasing function of Ω for every value of Pr, as is shown in Fig. 3, where the modulus of $f_{1b}^* Re$ is plotted versus Ω for $Pr = 0.7$, 7 and 100, in the range $0 \leqslant \Omega \leqslant 100$. On the other hand, the amplitude of the oscillations of $f_2 Re^2/Gr$, i.e. $|f_{2b}^* Re|$, is not a decreasing function of Ω. For a given value of the Prandtl number there exists a value of Ω which maximizes the modulus of $f_{2b}^* Re$ and thus represents a resonance frequency for the oscillations of the friction factor at the wall $Y = L$. This result is illustrated in Fig. 4, where the modulus of $f_{2b}^* Re$ is plotted versus Ω in the range $0 \leqslant \Omega \leqslant 100$, for $Pr = 0.7$, 7 and 100. The figure shows that the resonance frequency is a decreasing function of Pr and reaches a very low value for $Pr = 100$. Indeed, the values of the resonance frequency for the plots reported in Fig. 4 are, with an accuracy of four digits: $\Omega = 63.92$ for $Pr = 0.7$, $\Omega = 10.22$ for $Pr = 7$, $\Omega = 0.7440$ for $Pr = 100$. Table 1 provides resonance values of Ω which correspond to some values of Pr ranging from 0.3 to 1000. This table shows that the resonance value of Ω is not a monotonic function of Pr in the range $0.3 \leqslant Pr \leqslant 0.5$. It is interesting to note that no resonance frequency exists if $Pr < 0.277$. Indeed, if $Pr < 0.277$, $|f_{2b}^* Re|$ is a strictly decreasing function of Ω.

The Nusselt number represents the dimensionless heat flux per unit area through a vertical plane and is defined for every value of y. As is shown by Eqs. (35) and (36), the Nusselt number is composed of a steady part, Nu_a^*, which is a real constant, and an oscillating part whose amplitude is the modulus of the complex number Nu_b^*, which depends on y and on the product ΩPr. The time-averaged value of the Nusselt number coincides with Nu_a^*, and is independent of y.

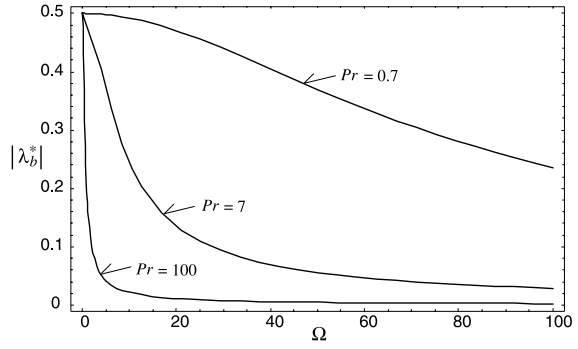

Fig. 2. Plots of the modulus of λ_b^* versus Ω in the range $0 \leqslant \Omega \leqslant 100$, for $Pr = 0.7$, 7 and 100.

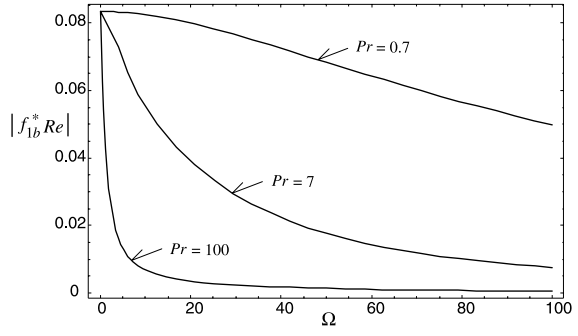

Fig. 3. Plots of the modulus of $f_{1b}^* Re$ versus Ω in the range $0 \leqslant \Omega \leqslant 100$, for $Pr = 0.7$, 7 and 100.

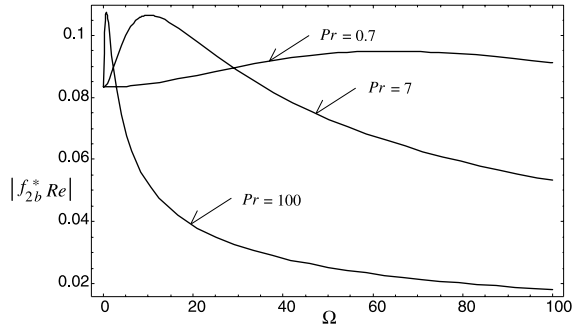

Fig. 4. Plots of the modulus of $f_{2b}^{*}Re$ versus Ω in the range $0 \leqslant \Omega \leqslant 100$, for $Pr = 0.7$, 7 and 100.

Table 1
Values of Ω which correspond to resonances of $f_2 Re$

Pr	Ω	Pr	Ω
0.3	55.92	1.2	45.98
0.32	66.65	1.5	39.17
0.34	71.89	2.0	31.33
0.36	74.61	3.0	22.27
0.38	75.93	4.0	17.23
0.4	76.43	5.0	14.03
0.5	73.78	10.0	7.253
0.6	68.85	20.0	3.680
0.7	63.92	50.0	1.484
0.8	59.44	100.0	0.7440
0.9	55.45	500.0	0.1491
1.0	51.92	1000.0	0.07456

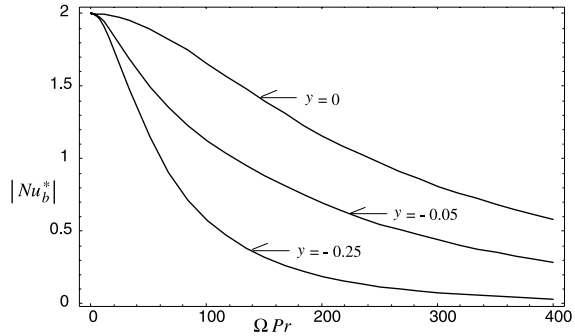

Fig. 5. Plots of the modulus of Nu_b^{*} versus ΩPr in the range $0 \leqslant \Omega Pr \leqslant 400$, for $y = -0.25$, -0.05 and 0.

The modulus of Nu_b^{*} at the steady-temperature wall ($y = -0.25$), at $y = -0.05$, and at the midplane of the channel ($y = 0$) is plotted versus ΩPr in Fig. 5, in the range $0 \leqslant \Omega Pr \leqslant 400$. As is illustrated by this figure, the amplitude of the oscillations of the Nusselt number is a decreasing function of ΩPr in the whole interval $-0.25 \leqslant y \leqslant 0$. On the contrary, in the open interval $0 < y < 0.25$, for every value of y there exists a value of ΩPr which maximizes the modulus of Nu_b^{*}, i.e. there exists a resonance frequency for the fluctuations of the Nusselt number which is proportional to the inverse of Pr. In this interval, the value of ΩPr which maximizes the modulus of Nu_b^{*} is an increasing function of y. Finally, at the right wall, the modulus of Nu_b^{*} is an increasing function of ΩPr, and no resonance occurs. These phenomena are illustrated in Figs. 6 and 7. In Fig. 6, plots of the modulus of Nu_b^{*} versus ΩPr are reported in the range $0 \leqslant \Omega Pr \leqslant 1200$, for $y = 0.1$, 0.17 and 0.2. For the plots reported in Fig. 6, the resonance frequencies correspond to $\Omega Pr = 93.61$, 312.7 and 800.0. In Fig. 7, plots of the modulus of Nu_b^{*} versus ΩPr are reported in the range $0 \leqslant \Omega Pr \leqslant 40{,}000$, for $y = 0.22$,

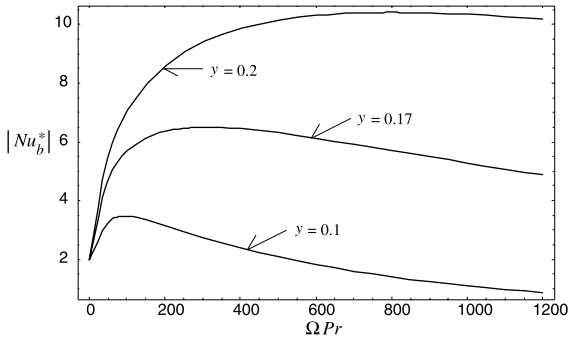

Fig. 6. Plots of the modulus of Nu_b^* versus ΩPr in the range $0 \leqslant \Omega Pr \leqslant 1200$, for $y = 0.1$, 0.17 and 0.2.

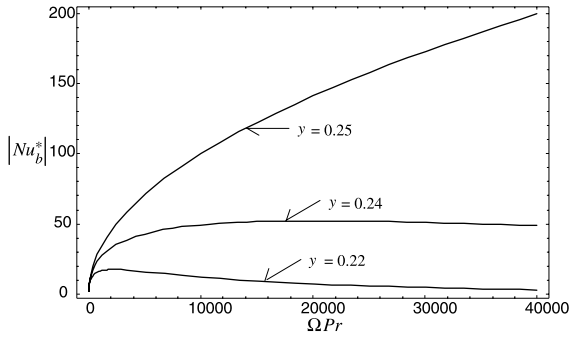

Fig. 7. Plots of the modulus of Nu_b^* versus ΩPr in the range $0 \leqslant \Omega Pr \leqslant 40{,}000$, for $y = 0.22$, 0.24 and 0.25.

Table 2
Values of the product ΩPr which correspond to resonances of Nu

y	ΩPr	y	ΩPr
0.005	13.27	0.13	135.3
0.01	30.40	0.14	162.6
0.015	38.75	0.15	199.3
0.02	44.60	0.16	247.3
0.025	49.19	0.17	312.7
0.03	53.03	0.18	408.1
0.04	59.40	0.19	555.6
0.06	69.82	0.2	800.0
0.08	80.16	0.21	1250.0
0.1	93.61	0.22	2222.2
0.11	103.2	0.23	5000.0
0.12	116.3	0.24	20000.0

0.24, and 0.25 (right wall). The first plot presents a resonance frequency for $\Omega Pr = 2222$, the second presents a resonance frequency for $\Omega Pr = 20{,}000$, while the third presents no resonance. Table 2 provides resonance values of the product ΩPr for the Nusselt number, in the open interval $0 < y < 0.25$. This table shows that the resonance value of ΩPr increases monotonically with y.

5. Discussion of the results: velocity and temperature distributions

The steady part u_a^* of the dimensionless velocity is a real function of y which agrees with the dimensionless velocity profile obtained in the analysis of the steady case [1,5,9].

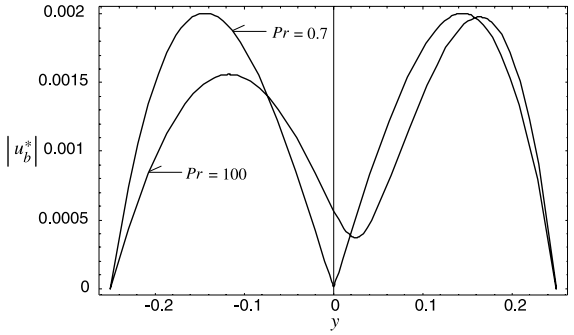

Fig. 8. Plots of the modulus of u_b^* versus y with $\Omega = 1$, for $Pr = 0.7$ and 100.

The oscillating part is proportional to Gr/Re and to the complex function u_b^*. Obviously, the modulus of $(Gr/Re)u_b^*$ coincides with the amplitude of the local dimensionless-velocity oscillations. Plots of $|u_b^*|$ versus y for $\Omega = 1$ are reported in Fig. 8, for $Pr = 0.7$ and 100. The plot for $Pr = 7$ is not reported because, for $\Omega \leqslant 1$, it is indistinguishable from that for $Pr = 0.7$. The figure shows that, for $Pr = 0.7$, the amplitude of the dimensionless velocity oscillations is almost exactly symmetric with respect to the midplane of the channel, is very close to zero at the midplane, and has two maxima for $y = -0.1443$ and 0.1443. On the other hand, for $Pr = 100$, the amplitude of the dimensionless velocity oscillations is not symmetric with respect to the midplane and differs appreciably from zero at this plane. Plots of the modulus of u_b^* versus y for $\Omega = 10$ are reported in Fig. 9, for $Pr = 0.7$, 7 and 100. The plot for $Pr = 0.7$ in Fig. 9 is very similar to that for the same value of Pr and $\Omega = 1$, reported in Fig. 8. The plot for $Pr = 7$ in Fig. 9 is similar to the plot in Fig. 8 which refers to $\Omega = 1$ and $Pr = 100$. The plot for $Pr = 100$ presents an average value much lower than that of

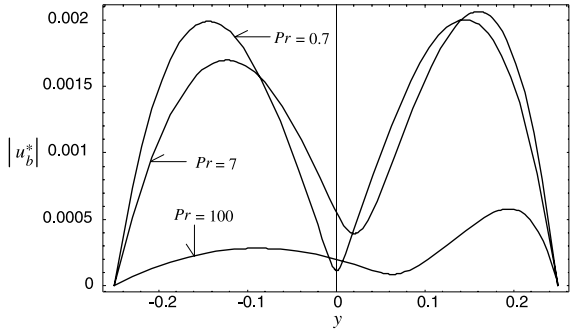

Fig. 9. Plots of the modulus of u_b^* versus y with $\Omega = 10$, for $Pr = 0.7$, 7 and 100.

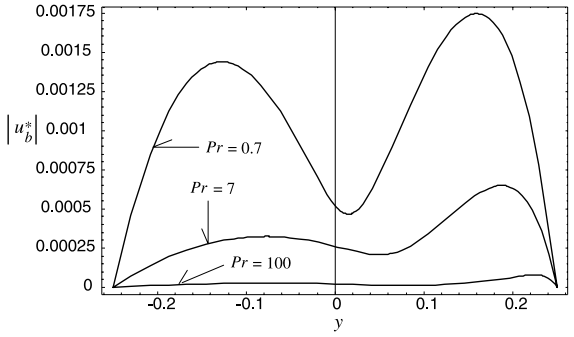

Fig. 10. Plots of the modulus of u_b^* versus y with $\Omega = 100$, for $Pr = 0.7$, 7 and 100.

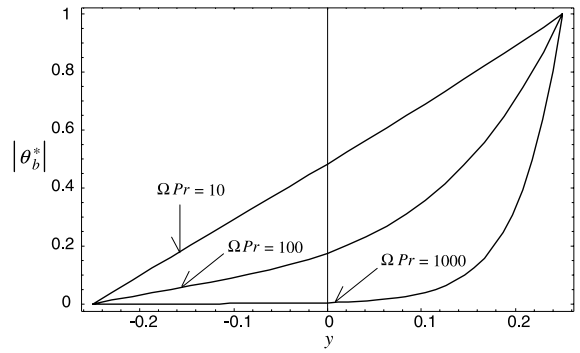

Fig. 11. Plots of the modulus of θ_b^* versus y for $\Omega Pr = 10$, 100 and 1000.

the other plots of the figure, and an absolute maximum rather close to the oscillating-temperature wall ($y = 0.1946$). Finally, plots of the modulus of u_b^* versus y for $\Omega = 100$ are reported in Fig. 10, for $Pr = 0.7$, 7 and 100. The figure shows that, for $\Omega = 100$, the amplitude of the dimensionless velocity oscillations is a strongly decreasing function of Pr at any position, obviously except at the walls, where velocity oscillations cannot occur. In particular, for $Pr = 100$ the amplitude of the velocity oscillations is very low throughout the channel.

As is shown by Eq. (27), the steady part θ_a^* of the dimensionless temperature is a real linear function of y, as in the steady case [1,5,9]. The oscillating part is proportional to θ_b^*, which, as is shown by Eq. (28), is a complex function of y and of the product ΩPr. Plots of the modulus of θ_b^* versus y for $\Omega Pr = 10$, 100 and 1000 are reported in Fig. 11. The figure shows that, for $\Omega Pr \leqslant 10$, the amplitude of the temperature oscillations looks like a linear function of y. On the other hand, when the value of ΩPr becomes higher and higher, the temperature oscillations tend to be sensible only in a narrow region of the channel adjacent to the wall $Y = L$.

6. Conclusions

The steady-periodic mixed convection in an inclined parallel-plate channel has been investigated by an analytical solution of the governing balance equations, under the following assumptions: the flow is laminar and parallel, the heat flux is transverse to the flow. It has been pointed out that the latter assumption is compatible with the thermal boundary conditions prescribed: both walls have a uniform temperature, which is stationary on one wall and sinusoidally time-varying on the other wall. The temperature distribution has been evaluated by solving the energy balance equation; then it has been substituted in the momentum balance equation. The solution of the latter equation has provided both the velocity distribution and the streamwise pressure drop. It has been shown that four dimensionless parameters must be fixed to determine the solution: the ratio between the Grashof number and the Reynolds number Gr/Re, the Prandtl number Pr, the temperature difference ratio χ and the dimensionless frequency Ω.

The most interesting features of the solution are the following:

- The oscillation amplitude of the dimensionless local velocity can be expressed as $|Gr/Re||u_b^*|$, where $|u_b^*|$ is a function of Pr, Ω and of the position y. The oscillation amplitude of the dimensionless pressure drop is given by $|Gr/Re||\lambda_b^*|$, where $|\lambda_b^*|$ is a function of Pr and Ω. The oscillation amplitude of the dimensionless local temperature can be expressed as a function of the product ΩPr and of the position y. Since Ω and Pr do not depend on the average fluid velocity U_0, all the above mentioned amplitudes are independent of the mean flow direction ($U_0 > 0$ or $U_0 < 0$).
- For every value of Pr, the oscillation amplitudes of the dimensionless pressure drop λ and of the friction factor $f_1 Re$ decrease monotonically with Ω. On the other hand, if $Pr \geqslant 0.277$, the oscillation amplitude of the friction factor $f_2 Re$ is not a monotonic function of Ω and a resonance frequency exists for any given value of Pr. If $Pr < 0.277$, the oscillation amplitude of the friction factor $f_2 Re$ decreases monotonically with Ω.
- The oscillation amplitude of dimensionless heat flux, i.e. of the Nusselt number Nu, depends on the dimensionless coordinate y and on the product ΩPr. If $-0.25 < y < 0$, i.e. in the half-channel next to the steady-temperature wall, the oscillation amplitude of Nu is a monotonically decreasing function of ΩPr. On the other hand, if $0 < y < 0.25$, i.e. in the half-channel next to the oscillating-temperature wall, the oscillation amplitude of Nu is not a monotonic function of ΩPr, and a resonance value of ΩPr exists for any given y.

References

[1] W. Aung, G. Worku, Theory of fully developed combined convection including flow reversal, ASME J. Heat Transfer 108 (1986) 485–488.
[2] C.H. Cheng, H.S. Kou, W.H. Huang, Flow reversal and heat transfer of fully developed mixed convection in vertical channels, J. Thermophys. Heat Transfer 4 (1990) 375–383.
[3] T.T. Hamadah, R.A. Wirtz, Analysis of laminar fully developed mixed convection in a vertical channel with opposing buoyancy, ASME J. Heat Transfer 113 (1991) 507–510.
[4] A.S. Lavine, Analysis of fully developed opposing mixed convection between inclined parallel plates, Wärme-und Stoffübertragung 23 (1988) 249–257.
[5] A. Barletta, E. Zanchini, On the choice of the reference temperature for fully-developed mixed convection in a vertical channel, Int. J. Heat Mass Transfer 42 (1999) 3169–3181.
[6] A. Barletta, Laminar mixed convection with viscous dissipation in a vertical channel, Int. J. Heat Mass Transfer 41 (1998) 3501–3513.
[7] A. Barletta, Analysis of combined forced and free flow in a vertical channel with viscous dissipation and isothermal–isoflux boundary conditions, ASME J. Heat Transfer 121 (1999) 349–356.
[8] A. Barletta, Heat transfer by fully developed flow and viscous heating in a vertical channel with prescribed wall heat fluxes, Int. J. Heat Mass Transfer 42 (1999) 3873–3885.
[9] A. Barletta, E. Zanchini, Mixed convection with viscous dissipation in an inclined channel with prescribed wall temperatures, Int. J. Heat Mass Transfer 44 (2001) 4267–4275.
[10] M. Kazmierczak, Z. Chinoda, Buoyancy-driven flow in an enclosure with time periodic boundary conditions, Int. J. Heat Mass Transfer 35 (1992) 1507–1518.
[11] H.S. Kwak, K. Kuwahara, J.M. Hyun, Resonant enhancement of natural convection heat transfer in a square enclosure, Int. J. Heat Mass Transfer 41 (1998) 2837–2846.
[12] J.L. Lage, A. Bejan, The resonance of natural convection in an enclosure heated periodically from the side, Int. J. Heat Mass Transfer 36 (1993) 2027–2038.
[13] B.V. Antohe, J.L. Lage, Amplitude effect on convection induced by time periodic horizontal heating, Int. J. Heat Mass Transfer 39 (1996) 1121–1133.